

Short Note

2-[2,6-Diisopropylphenyl]-4-phenyl-5*H*-5,9*b*[1',2']-benzonaphtho[1,2-*b*]pyrrol-2-ium Tetrafluoroborate

Masaru Tanaka, Shota Kamiyama, Akihiko Ishii and Norio Nakata * 

Department of Chemistry, Graduate School of Science and Engineering, Saitama University,
255 Shimo-okubo, Sakura-ku, Saitama 338-8570, Japan

* Correspondence: nakata@chem.saitama-u.ac.jp; Tel.: +81-48-858-3392

Abstract: A novel α,β -unsaturated iminium salt (**3**) incorporated into a rigid dibenzobarrelene backbone was synthesized by heating *N*-(anthracen-9-ylmethyl)-2,6-diisopropylaniline (**2**) and 3-phenyl-2-propynal in THF in the presence of excess amounts of magnesium sulfate and 0.5 equivalents of an HBF₄-Et₂O complex. The molecular structure of **3** was characterized unambiguously by NMR spectroscopy and single-crystal X-ray diffraction (SCXRD) analyses. Compound **3** exhibits yellow luminescence in CH₂Cl₂ ($\lambda_{em} = 516$ nm) and in the solid state ($\lambda_{em} = 517$ nm) with relatively high to moderate quantum yields ($\Phi_{F(CH_2Cl_2)} = 0.63$; $\Phi_{F(solid)} = 0.34$).

Keywords: α,β -unsaturated iminium salt; dibenzobarrelene; luminescence; single-crystal X-ray diffraction analysis

1. Introduction

The condensation of carbonyl compounds such as aldehydes or ketones with a primary amine typically results in an equilibrium where a substantial amount of imine is present. In contrast, when a secondary amine is employed, the aldehyde may condense to form an iminium ion, which, owing to the absence of a deprotonation step, can only be isolated as a salt of a strong acid [1,2]. For example, cyanine derivatives containing α,β -unsaturated iminium moieties are currently widely used not only as functional materials, such as dyes for optical recording media [3,4], but also as bio-imaging dyes [5–7]. However, the synthesis of an iminium salt that emits strongly both in solution and in the solid state is extremely rare [8]. Meanwhile, we are conducting an investigation into the synthesis of a series of 1,4-diaryl-1,3-butadiene derivatives that are incorporated into a rigid dibenzobarrelene backbone, wherein both components share each ethene unit and the 1 position of the 1,3-butadiene unit is linked to the bridgehead of the dibenzobarrelene by a main group element (Figure 1) [9–13]. These derivatives exhibit high fluorescence efficiency in solution and in the solid state due to the conformationally fixed 1,4-diaryl-1,3-butadiene fluorophore and the sterically bulky dibenzobarrelene moiety, which prevent intramolecular interactions. Herein, we present the synthesis, structure, and photophysical properties of an α,β -unsaturated iminium salt fixed in a dibenzobarrelene skeleton.

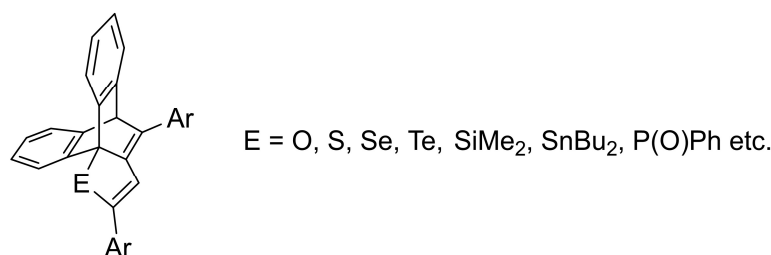


Figure 1. 1,4-diaryl-1,3-butadiene derivatives bearing a rigid dibenzobarrelene backbone.



Citation: Tanaka, M.; Kamiyama, S.; Ishii, A.; Nakata, N.

2-[2,6-Diisopropylphenyl]-4-phenyl-5*H*-5,9*b*[1',2']-benzonaphtho[1,2-*b*]pyrrol-2-ium Tetrafluoroborate.

Molbank **2023**, *2023*, M1601.

<https://doi.org/10.3390/M1601>

Academic Editor: René T. Boéré

Received: 2 February 2023

Revised: 3 March 2023

Accepted: 8 March 2023

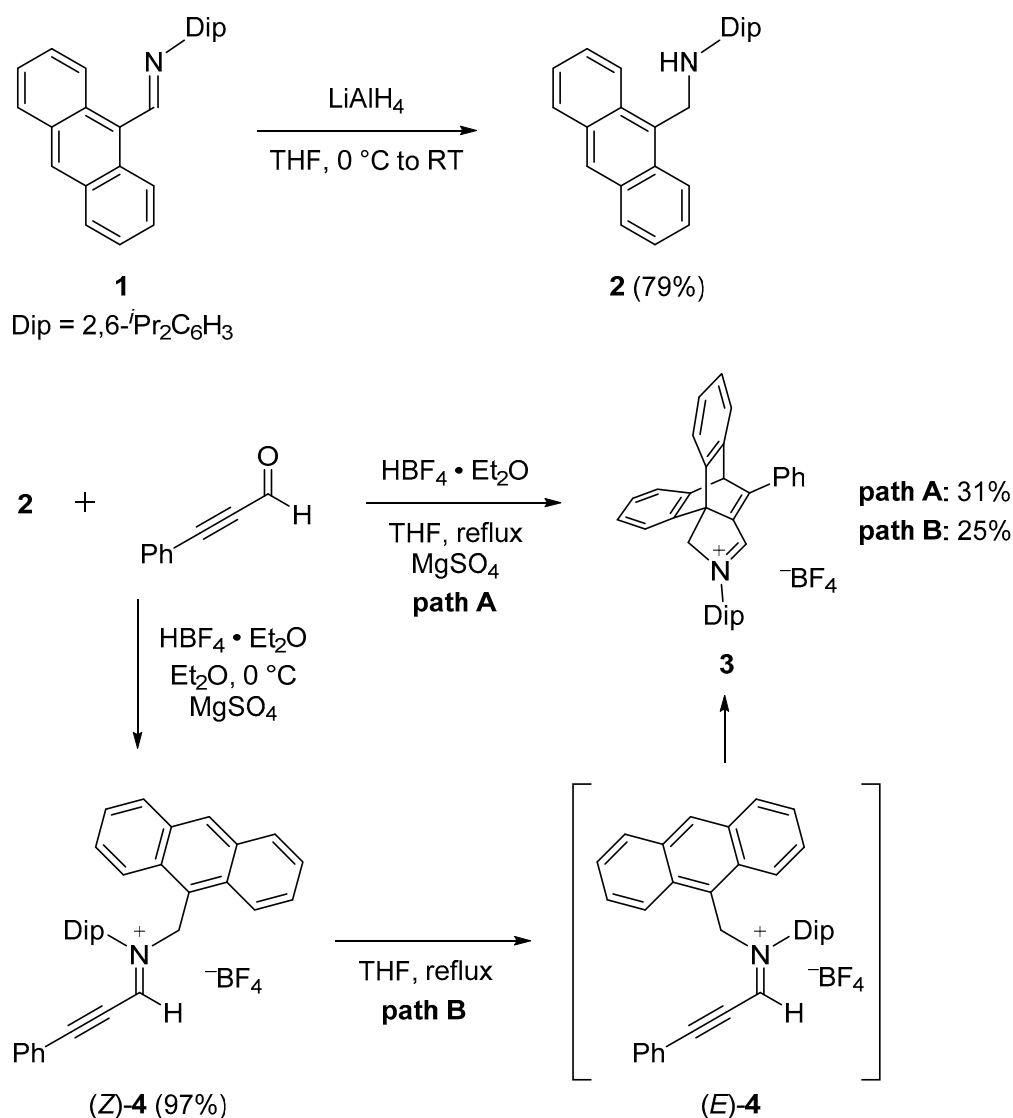
Published: 10 March 2023



Copyright: © 2023 by the authors. Licensee MDPI, Basel, Switzerland. This article is an open access article distributed under the terms and conditions of the Creative Commons Attribution (CC BY) license (<https://creativecommons.org/licenses/by/4.0/>).

2. Results and Discussion

N-(Anthracen-9-ylmethyl)-2,6-diisopropylaniline (**2**) was prepared as yellow crystals in 79% yield by the reduction of the starting imine *N*-(9-anthracenylmethylene)-2,6-bis(1-methylethyl)benzenamine (**1**) [14] with LiAlH_4 in THF at 0 °C (Scheme 1). The target iminium salt (**3**) was successfully synthesized as yellow crystals in 31% yield by refluxing a THF solution of 3-phenyl-2-propynal [15] and the amine (**2**) in the presence of excess amounts of magnesium sulfate and 0.5 equivalents of an $\text{HBF}_4\cdot\text{Et}_2\text{O}$ complex (Scheme 1, Path A). The structure of **3** was characterized through the following spectroscopic analyses: In the ^1H NMR spectrum of **3** in CDCl_3 , the methine and methylene protons at the bridgehead positions were observed as a singlet signal at 6.08 and 5.49 ppm, respectively. The methyl protons of the isopropyl groups on the Dip group showed doublet signals at 1.26 and 1.44 ppm, while a septet signal due to the methine proton resonated at 2.67 ppm. The iminium proton (9.20 ppm) appeared in a characteristic low-field region, which is comparable to that of the related five-membered iminium salt (9.48 ppm) [16]. In the $^{13}\text{C}\{^1\text{H}\}$ NMR spectrum of **3**, the iminium carbon is observed at 172.1 ppm. Furthermore, the $^{11}\text{B}\{^1\text{H}\}$ NMR spectrum of **3** displayed a signal at -1.14 ppm, suggesting that the $[\text{BF}_4]^-$ anion exists as a free counter anion in solution.



Scheme 1. Synthesis of the iminium salt (**3**).

Single crystals of **3** were obtained by slow evaporation of its CH_2Cl_2 solution at room temperature, and the molecular structure was determined by a single-crystal X-ray diffraction (SCXRD) analysis. The iminium salt (**3**) crystallizes in the monoclinic space group $P2_1/n$ with one H_2O molecule and $[\text{BF}_4]^-$ anion in the asymmetric unit. Given that **3** was recrystallized under atmospheric conditions, it is probable that the H_2O molecule was incorporated into the unit cell of **3** during crystallization. The ORTEP is shown in Figure 2, and the relevant geometrical parameters are summarized in Table 1. The distance between H3 ... O1 is 2.1845(17) Å, which is shorter than the sum of the van der Waals radii of the two atoms (2.60 Å) [17], indicating the presence of hydrogen bonding in the unit cell. In contrast to the related 2*H*-pyrrolium salts [18–23], it is exceptional for the H_2O molecule to engage in hydrogen bonding with the C–H bond of the iminium fragment. This is likely due to the steric hindrance surrounding the iminium fragment and the highly acidic iminium proton, which serves as a donor to the H_2O molecule. The intermolecular hydrogen bonds involving lattice water molecules and BF_4^- ions were also confirmed in the crystal packing of **3**. The non-bonded OH ... F distances (H35* ... F4 and H36* ... F4) are 1.88(2) and 2.12(2), which can be regarded as a relatively strong interaction [24]. The distance between the nitrogen atom (N1) in the iminium moiety and the counter anion (B1 ... N1) is 5.194(2) Å, which is considerably longer than the sum of the van der Waals radii of the two atoms (3.84 Å) [17], suggesting that the iminium moiety exists as a free cation in the crystalline state. The C=N [1.308(2) Å], C–N [1.484(2) Å], and C–C bond lengths [1.409(2)–1.547(3) Å] in the five-membered ring are similar to those of the reported 2*H*-pyrrolium salts [18–23]. Furthermore, the dihedral angle of the conjugated moiety comprising N1–C3–C4–C5 is almost 180° as a result of its incorporation into a rigid framework. The torsion angle (C4–C5–C31–C32) between the alkenyl moiety and the benzene ring attached to the C5 carbon is $-153.38(17)^\circ$, which falls within the range of values observed in related dibenzobarrelene-incorporated 1,3-butadiene derivatives [8], thus forming an effective conjugated system. In contrast, the dihedral angle (C3–N1–C19–C20) comprising the benzene ring in the Dip group and the imine moiety is $-77.0(2)^\circ$, which is nearly perpendicular due to the bulkiness of the Dip group.

The formation of **3** can be explained by the intramolecular Diels–Alder reaction of iminium intermediate **4**. To verify this supposition, we attempted the direct synthesis of **4**. Upon reacting **2** with 3-phenyl-2-propynal in the presence of an excess amount of magnesium sulfate and an $\text{HBF}_4\text{-Et}_2\text{O}$ complex at 0 °C in Et_2O , the corresponding (*Z*)-**4** was obtained in an almost quantitative yield as red crystals (Scheme 1, Path B). In the ^1H NMR spectrum of (*Z*)-**4**, the iminium proton was observed at 9.86 ppm, which showed a somewhat down-field shift compared to that of **3** (9.20 ppm). The molecular structure of (*Z*)-**4** was finally confirmed by SCXRD (see Supplementary Materials). Subsequently, the intramolecular cyclization reaction, accompanied by the isomerization from (*Z*)-**4** to (*E*)-**4**, proceeded under refluxing conditions in THF, resulting in the formation of the corresponding **3** in a 25% yield.

Interestingly, the iminium salt (**3**) exhibited yellow fluorescence in CH_2Cl_2 solution and in the solid state. The UV–visible absorption spectrum of **3** in CH_2Cl_2 shows two absorption bands, with the longest absorption maximum (λ_{abs}) at 423 nm and a molar absorption coefficient ϵ of $9820 \text{ M}^{-1} \text{ cm}^{-1}$ (Figure 3a, Table 2). On the other hand, the fluorescence spectrum of **3** in CH_2Cl_2 has a maximum wavelength (λ_{em}) of 516 nm with a Stokes shift of 4300 cm^{-1} (152 nm). We reported the Stokes shifts of the 1,3-butadiene derivatives incorporated into the dibenzobarrelene skeleton in the range of $4700\text{--}6100 \text{ cm}^{-1}$ [9], which are larger than those of **3**. This result suggests that the structure change in the excited state of **3** is small compared with those derivatives. The fluorescence quantum yield Φ_{F} has a relatively high value of 0.63. Furthermore, the λ_{em} of **3** in the solid state was observed at 517 nm, which is almost the same as that in the CH_2Cl_2 solution. The Φ_{F} of **3** in the solid state was 0.34, which was significantly lower than that in the solution.

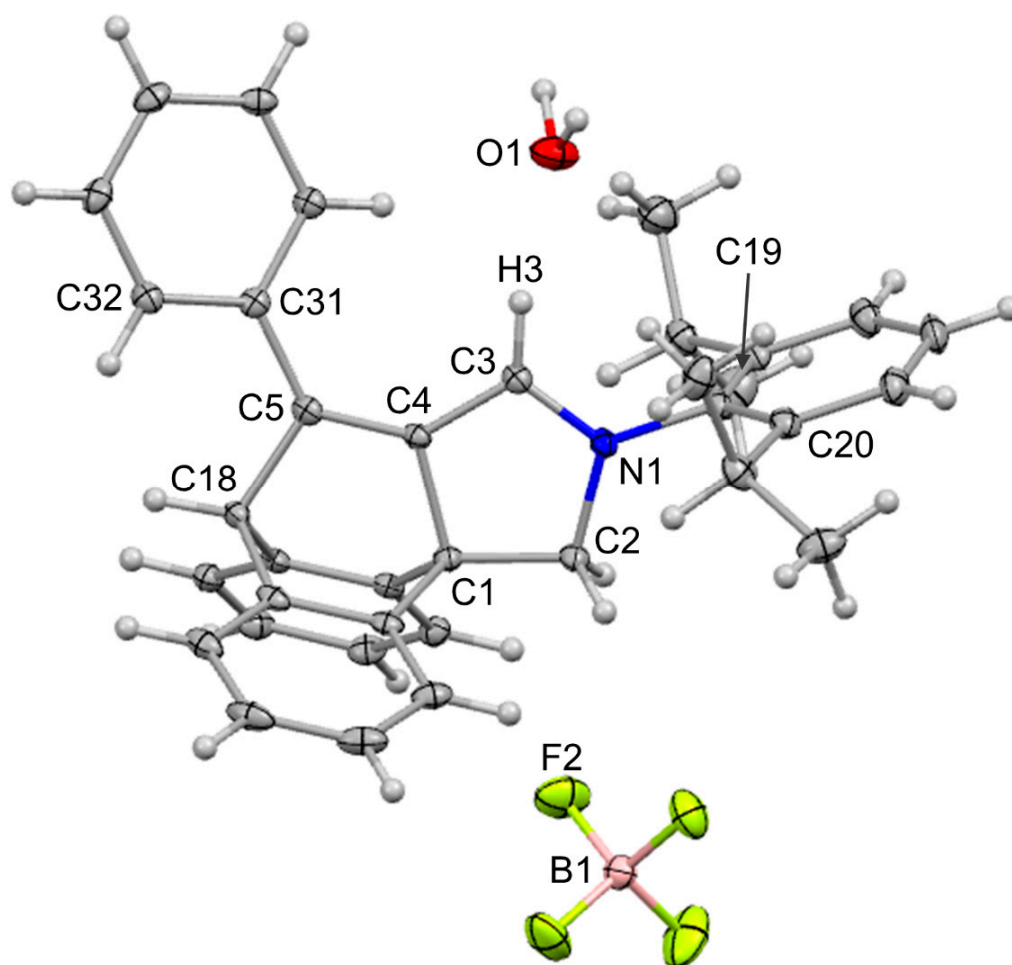


Figure 2. ORTEP of 3·H₂O with thermal ellipsoids at 50% probability.

Table 1. Selected bond lengths [Å] and bond angles [°].

Bond Lengths	[Å]	Bond Angles	[°]
C4–C5	1.355(2)	N1–C3–C4	111.67(16)
C3–C4	1.409(2)	C3–C4–C1	107.34(15)
C3–N1	1.308(2)	C3–C4–C5	135.48(16)
C2–N1	1.484(2)	C1–C4–C5	117.10(15)
C1–C2	1.521(2)	C4–C5–C18	110.06(15)
C1–C4	1.547(3)	C31–C5–C4	128.92(16)
H3 ... O1	2.1845(17)	C3–N1–C19–C20	−77.0(2)
B1 ... N1	5.194(2)	C4–C5–C31–C32	−153.38(17)
		N1–C3–C4–C5	179.34(18)

Table 2. Photophysical data for 3^a.

λ_{abs} [nm]	ϵ [M ^{−1} cm ^{−1}]	λ_{em} (CH ₂ Cl ₂) [nm]	Stokes Shift [cm ^{−1}] (nm)	Φ_{F} (CH ₂ Cl ₂) ^b	λ_{em} (solid) [nm]	Φ_{F} (Solid) ^b
423	9820	516	4300 (152)	0.63	517	0.34

^a 1 × 10^{−5} M in CH₂Cl₂ at room temperature under argon. ^b The absolute fluorescence quantum yields were determined using a calibrated integrating sphere system.

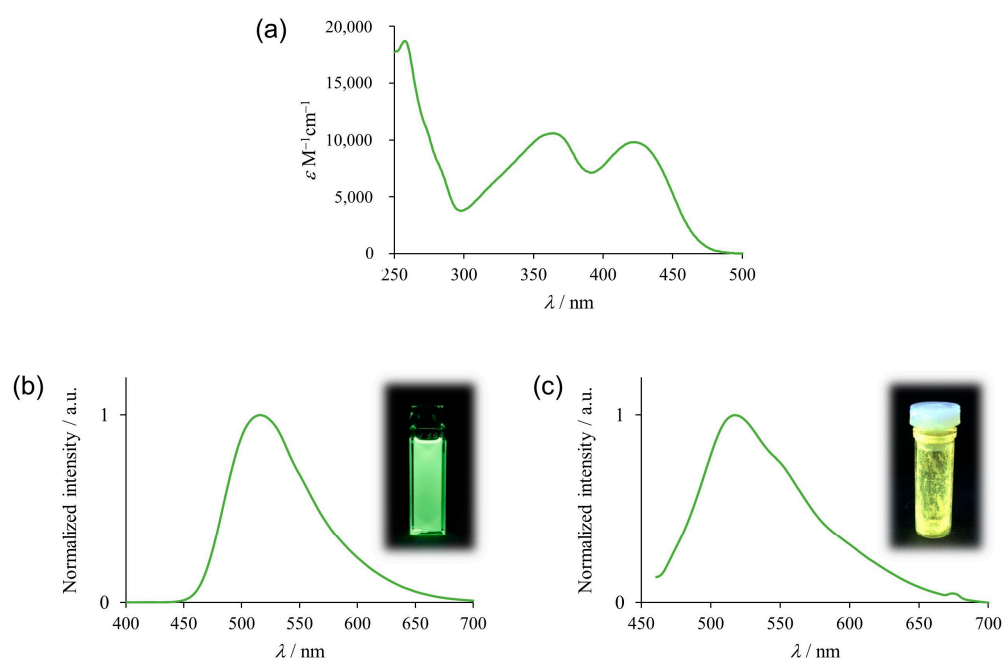


Figure 3. (a) Optical absorption spectrum of **3** in CH_2Cl_2 , (b) fluorescence spectrum of **3** in CH_2Cl_2 , and (c) fluorescence spectrum of **3** in the solid state, with photographs under irradiation with light ($\lambda = 364$ nm).

3. Materials and Methods

3.1. General Considerations

Unless otherwise noted, all experiments were carried out under an argon atmosphere using standard Schlenk-line techniques. The ^1H and ^{13}C spectra were recorded on a Bruker AVANCE-400 (400 and 101 MHz, respectively) or a Bruker AVANCE-500 (500 and 126 MHz, respectively) spectrometer using CDCl_3 as the solvent at room temperature. The ^{11}B and ^{19}F NMR spectra were recorded on a Bruker AVANCE-500 (160 and 471 MHz, respectively) spectrometer using CDCl_3 as the solvent at room temperature. The UV-vis spectra were recorded on a U-1900 spectrophotometer (HITACHI Co., Ltd., Hitachi, Japan). The fluorescence spectra were recorded on FP-6600 and FP-6300 spectrofluorimeters (JASCO Corp., Tokyo, Japan). The absolute photoluminescence quantum yields were measured using the calibrated integrating sphere system C10027 (Hamamatsu Photonics Co. Ltd., Hamamatsu City, Japan). The elemental analyses were carried out at the Comprehensive Analysis Center for Science, Saitama University. The thermogravimetry (TG) analysis was carried out using a NETZSCH analyzer, the STA2500, as follows: under a helium atmosphere with a temperature range of 25–300 °C and a heating rate of 10 °C /min. All melting points were determined on a Mel-Temp capillary tube apparatus and are uncorrected. All solvents were dried over 4A molecular sieves or a potassium mirror before use. All materials were obtained from commercial suppliers and used without further purification, except for *N*-(9-anthracenylmethylene)-2,6-bis(1-methylethyl)benzenamine (**1**) [14] and 3-phenyl-2-propynal [15], which were prepared according to their respective literature procedures.

3.2. Synthesis of *N*-(Anthracen-9-ylmethyl)-2,6-diisopropylaniline (**2**)

A total of 321 mg of LiAlH_4 (8.47 mmol) was added to a solution of **1** (2.05 g; 5.64 mmol) in THF (50 mL) at 0 °C. Subsequently, the temperature was raised to room temperature over a period of 4 h. After cooling the solution to 0 °C, 1 M NaOH aq. was added. The suspension was filtered through a pad of Celite®. The mixture was extracted with Et_2O , and the extract was washed with water, dried over anhydrous Na_2SO_4 , and evaporated to dryness. The residue was washed with a small amount of hexane (ca. 10 mL) and dried under reduced pressure to provide pure **2** (1.63 g; 79%) as yellow crystals. Mp. 147–148 °C.

^1H NMR (400 MHz; 25 °C; CDCl_3): δ = 1.16 (d, J = 6.8 Hz, 12H), 3.25 (sept, J = 6.8 Hz, 2H), 3.32 (s, 1H), 5.04 (s, 2H), 7.09–7.13 (m, 3H, Ar), 7.46–7.51 (m, 4H, Ar), 8.03 (d, J = 8.4 Hz, 2H, Ar), 8.30 (d, J = 8.4 Hz, 2H, Ar), 8.45 (s, 1H, Ar). $^{13}\text{C}\{^1\text{H}\}$ NMR (101 MHz, 25 °C, CDCl_3): δ = 24.2 (2 CH_3), 28.0 (CH), 48.1 (CH_2), 123.58 (CH), 123.68 (CH), 124.4 (CH), 126.0 (CH), 127.5 (CH), 129.0 (CH), 130.2 (C), 131.6 (2 C), 141.8 (C), 144.1 (C). Anal. Calcd. For $\text{C}_{27}\text{H}_{28}\text{N}$: C, 88.48; H, 7.77; N, 3.82. Found: C, 88.22; H, 7.68; N, 3.77.

3.3. Synthesis of 2-[2,6-Diisopropylphenyl]-4-phenyl-5h-5,9b[1',2']-benzophthol[1,2-b]pyrrol-2-ium Tetrafluoroborate (3)

A complex of $\text{HBF}_4\text{-Et}_2\text{O}$ (0.0204 M; 0.13 mL; 0.75 mmol) was added dropwise to a solution of 3-phenyl-2-propynal (0.179 mL; 193 mg; 1.51 mmol), **2** (554.4 mg; 1.51 mmol), and MgSO_4 (110 mg) in anhydrous THF (70 mL) at 0 °C. The mixture was heated under reflux overnight. The suspension was filtered through a pad of Celite®. After evaporation, the residue was reprecipitated from CH_2Cl_2 /benzene to provide pure **3** as yellow crystals (428 mg; 31%). Mp. 276–278 °C (dec.). ^1H NMR (400 MHz; 25 °C; CDCl_3): δ = 1.26 (d, J = 6.5 Hz, 6H), 1.44 (d, J = 6.5 Hz, 6H), 2.67 (sept, J = 6.5 Hz, 2H), 5.49 (s, 2H, CH_2), 6.08 (s, 1H, CH), 7.21–7.29 (m, 4H, Ar), 7.38 (d, J = 7.5 Hz, 4H, Ar), 7.56–7.64 (m, 6H, Ar), 7.79 (d, J = 7.5 Hz, 2H, Ar), 9.20 (s, 1H). $^{13}\text{C}\{^1\text{H}\}$ NMR (126 MHz, 25 °C, CDCl_3): δ = 19.2 (CH_3), 24.3 (CH_3), 24.8 (CH_3), 27.3 (CH), 29.1 (CH_3), 29.7 (CH), 58.3 (CH), 58.9 (C), 61.0 (CH_2), 121.8 (CH), 125.3 (CH), 125.5 (CH), 127.2 (CH), 127.4 (CH), 127.6 (CH), 127.8 (CH), 128.1 (CH), 128.6 (CH), 130.3 (CH), 132.2 (CH), 132.9 (CH), 133.3 (CH), 133.8 (CH), 141.0 (C), 142.2 (C), 143.3 (C), 143.4 (C), 167.1 (CH), 172.1 (C). $^{11}\text{B}\{^1\text{H}\}$ NMR (160 MHz, 25 °C, CDCl_3): δ = −1.14 (s). $^{19}\text{F}\{^1\text{H}\}$ NMR (471 MHz, 25 °C, CDCl_3): δ = −153.1 (s).

3.4. Synthesis of (Z)-Anthracenyl-9-methyl-(2,6-diisopropylphenyl)-(3-phenylprop-2-ynylidene)ammonium Tetrafluoroborate [(Z)-4]

A complex of $\text{HBF}_4\text{-Et}_2\text{O}$ (0.0204 M, 0.07 mL, 0.41 mmol) was added dropwise to a solution of 3-phenyl-2-propynal (0.096 mL; 105.6 mg; 0.82 mmol), **2** (299.5 mg; 0.82 mmol), and MgSO_4 (60 mg) in anhydrous Et_2O (30 mL) at 0 °C. The mixture was stirred for 4 h at 0 °C. The suspension was filtered through a pad of Celite®. After evaporation, the residue was washed with hexane (ca. 10 mL) to provide pure (Z)-**4** as red crystals (753 mg; 97%). Mp. 150–151 °C (dec.). ^1H NMR (500 MHz; 25 °C; CDCl_3): δ = 0.45 (d, J = 6.7 Hz, 6H), 0.98 (d, J = 6.7 Hz, 6H), 2.39 (sept, J = 6.7 Hz, 2H), 6.50 (s, 2H), 7.11–7.12 (m, 2H, Ar), 7.20–7.21 (m, 2H, Ar), 7.32–7.35 (m, 2H, Ar), 7.42–7.55 (m, 6H, Ar), 7.87 (d, J = 7.7 Hz, 2H, Ar), 8.00 (d, J = 7.7 Hz, 2H, Ar), 8.53 (s, 1H, Ar), 9.86 (s, 1H). $^{13}\text{C}\{^1\text{H}\}$ NMR (126 MHz, 25 °C, CDCl_3): δ = 22.4 (CH_3), 25.5 (CH), 28.7 (CH), 59.9 (CH_2), 85.3 (C), 117.4 (C), 118.7 (C), 121.9 (CH), 124.3 (C), 125.2 (CH), 125.4 (CH), 128.3 (CH), 129.3 (CH), 129.6 (CH), 131.3 (C), 131.7 (CH), 131.79 (CH), 131.83 (CH), 134.4 (CH), 135.0 (C), 143.7 (C), 159.0 (CH). $^{11}\text{B}\{^1\text{H}\}$ NMR (CDCl_3 , 160 MHz): δ = −0.49 (s). $^{19}\text{F}\{^1\text{H}\}$ NMR (CDCl_3 , 471 MHz): δ = −152.0 (s).

3.5. SCXRD Analysis of 3

Yellow single crystals of **3** were grown by slow evaporation of its CH_2Cl_2 solution at room temperature. The intensity data were collected at 100 K on a Bruker SMART APEX II diffractometer employing graphite-monochromated $\text{MoK}\alpha$ radiation (λ = 0.71073 Å). The structure was solved by direct methods (SHELXT) [25] and refined by full-matrix least-squares procedures on F^2 for all reflections (SHELXL) [26]. The hydrogen atoms were located by assuming ideal geometry and included in the structure calculations without further refinement of the parameters.

The crystal data for $\text{C}_{36}\text{H}_{36}\text{BF}_4\text{NO}$ ($3\cdot\text{H}_2\text{O}$) are as follows: M = 585.47 g mol^{-1} , monoclinic, $P2_1/n$, a = 10.5927(15), b = 16.799(2), c = 17.106(2) Å, β = 100.067(2)°, V = 2997.2(7) Å³, Z = 4, D_x = 1.297 g cm^{-3} , $F(000)$ = 1232, and μ = 0.094 mm^{-1} . CCDC's deposition number is 2236656.

4. Conclusions

We have demonstrated the synthesis and characterization of a novel α,β -unsaturated iminium salt (**3**) incorporated into a rigid dibenzobarrelene skeleton. In CH_2Cl_2 solution and in the solid state, **3** showed yellow emission with relatively high to moderate quantum yields. Further applications using **3** are currently being investigated in our laboratory.

Supplementary Materials: The following are available online: All NMR spectra for **2** and **3** and crystallographic data for **3** in the Crystallographic Information File (CIF) format. CCDC 2236656 also contains the Supplementary Crystallographic Data for this paper.

Author Contributions: Conceptualization, M.T. and N.N.; methodology, N.N.; formal analysis, M.T. and S.K.; investigation, M.T. and S.K.; resources, N.N.; data curation, N.N.; writing—original draft preparation, M.T. and N.N.; writing—review and editing, A.I. and N.N.; visualization, N.N.; supervision, N.N. All authors have read and agreed to the published version of the manuscript.

Funding: This research was partially supported by JSPS KAKENHI (grant number: JP22K05138 to N.N.).

Data Availability Statement: CCDC 2236656 (**3**) contains the Supplementary Crystallographic Data for this paper. These data can be obtained free of charge via www.ccdc.cam.ac.uk/data_request/cif (accessed on 7 March 2023), by emailing data_request@ccdc.cam.ac.uk, or by contacting the Cambridge Crystallographic Data Centre, 12 Union Road, Cambridge CB2 1EZ, UK; fax: +44-1223-336033; e-mail: deposit@ccdc.cam.ac.uk.

Conflicts of Interest: The authors declare no conflict of interest.

References

1. Layer, R.W. The Chemistry of Imines. *Chem. Rev.* **1963**, *63*, 489–510. [[CrossRef](#)]
2. Erkkilä, A.; Majander, I.; Pihko, P.M. Iminium Catalysis. *Chem. Rev.* **2007**, *107*, 5416–5470. [[CrossRef](#)] [[PubMed](#)]
3. Emmelius, M.; Pawlowski, G.; Vollmann, H.W. Materials for Optical Data Storage. *Angew. Chem. Int. Ed. Engl.* **1989**, *28*, 1445–1471. [[CrossRef](#)]
4. Muströph, H.; Stollenwerk, M.; Bressau, V. Current Developments in Optical Data Storage with Organic Dyes. *Angew. Chem. Int. Ed.* **2006**, *45*, 2016–2035. [[CrossRef](#)]
5. Sun, W.; Guo, S.; Hu, C.; Fan, J.; Peng, X. Recent Development of Chemosensors Based on Cyanine Platforms. *Chem. Rev.* **2016**, *116*, 7768–7817. [[CrossRef](#)] [[PubMed](#)]
6. Ma, X.; Shi, L.; Zhang, B.; Liu, L.; Fu, Y.; Zhang, X. Recent advances in bioprobes and biolabels based on cyanine dyes. *Anal. Bioanal. Chem.* **2022**, *414*, 4551–4573. [[CrossRef](#)] [[PubMed](#)]
7. Pronkin, P.G.; Tatikolov, A.S. Photonics of Trimethine Cyanine Dyes as Probes for Biomolecules. *Molecules* **2022**, *27*, 6367. [[CrossRef](#)] [[PubMed](#)]
8. Tigreros, A.; Rosero, H.-A.; Castillo, J.-C.; Portilla, J. Integrated pyrazolo[1,5-*a*]pyrimidine-hemicyanine system as a colorimetric and fluorometric chemosensor for cyanide recognition in water. *Talanta* **2019**, *196*, 395–401. [[CrossRef](#)]
9. Ishii, A.; Nakata, N.J. Synthesis and Photophysical Property of 1-Chalcogeno-1,3-butadiene Derivatives and the Related Compounds Incorporated in a Dibenzobarrelene Skeleton. *Synth. Org. Chem. Jpn.* **2018**, *76*, 1042–1054. [[CrossRef](#)]
10. Ishii, A.; Shibata, M.; Ebina, R.; Nakata, N. Synthesis and Photophysical Properties of Dibenzobarrelene-Incorporated 1,4-Diphenyl-1,3-pentadienes and a 5-Sila Derivative Having High Fluorescence Efficiency. *Eur. J. Org. Chem.* **2018**, 1011–1018. [[CrossRef](#)]
11. Ishii, A.; Kikushima, C.; Hayashi, Y.; Ohtsuka, N.; Nakata, N.; Muranaka, A.; Tanaka, Y.; Uchiyama, M. 1-Phosphino-1,3-butadiene Derivatives Incorporated with Dibenzobarrelene Skeleton: Synthesis and Photophysical Properties. *Bull. Chem. Soc. Jpn.* **2020**, *93*, 1430–1442. [[CrossRef](#)]
12. Miyashita, Y.; Nakata, N.; Ishii, A. Synthesis and Properties of 1-(Dialkylstannyl)-1,4-diphenyl-1,3-butadiene Fused with a Dibenzobarrelene and the Corresponding Pentaorganostannate. *Z. Anorg. Allg. Chem.* **2021**, *647*, 1883–1889. [[CrossRef](#)]
13. Ishii, A.; Ebina, R.; Nakata, N. Formation, Chemical and Optical Properties of 1,2,5-Triphenylpentadienyl Cation Fixed in a Rigid Dibenzobarrelene Skeleton. *Eur. J. Org. Chem.* **2022**, *2022*, e202200033. [[CrossRef](#)]
14. Zhou, J.; Li, X.Y.; Sun, H.J. An efficient and recyclable water-soluble cyclopalladated complex for aqueous Suzuki reactions under aerial conditions. *J. Organomet. Chem.* **2010**, *695*, 297–303. [[CrossRef](#)]
15. Kuroda, H.; Hanaki, E.; Izawa, H.; Kano, M.; Itahashi, H. A convenient method for the preparation of α -vinylfurans by phosphine-initiated reactions of various substituted enynes bearing a carbonyl group with aldehydes. *Tetrahedron* **2004**, *60*, 1913–1920. [[CrossRef](#)]
16. Lavallo, V.; Canac, Y.; Präsang, C.; Donnadiou, B.; Bertrand, G. Stable Cyclic (Alkyl)(Amino)Carbenes as Rigid or Flexible, Bulky, Electron-Rich Ligands for Transition-Metal Catalysts: A Quaternary Carbon Atom Makes the Difference. *Angew. Chem., Int. Ed.* **2005**, *44*, 5705–5709. [[CrossRef](#)]

17. Bondi, A. van der Waals Volumes and Radii. *J. Phys. Chem.* **1964**, *68*, 441–451. [[CrossRef](#)]
18. Jazzar, R.; Dewhurst, R.D.; Bourg, J.-B.; Donnadiou, B.; Canac, Y.; Bertrand, G. Intramolecular “Hydroiminiumation” of Alkenes: Application to the Synthesis of Conjugate Acids of Cyclic Alkyl Amino Carbenes (CAACs). *Angew. Chem. Int. Ed.* **2007**, *46*, 2899–2902. [[CrossRef](#)]
19. Jazzar, R.; Dewhurst, R.D.; Bourg, J.-B.; Donnadiou, B.; Canac, Y.; Bertrand, G. Intramolecular “Hydroiminiumation and -Amidiniumation” of Alkenes: A Convenient, Flexible, and Scalable Route to Cyclic Iminium and Imidazolium Salts. *J. Org. Chem.* **2007**, *72*, 3492–3499. [[CrossRef](#)]
20. Dureen, M.A.; Brown, C.C.; Stephan, D.W. Addition of enamines or pyrroles and B(C₆F₅)₃ “Frustrated Lewis Pairs” to alkynes. *Organometallics* **2010**, *29*, 6422–6432. [[CrossRef](#)]
21. Smolobochkin, A.V.; Gazizov, A.S.; Melyashova, A.S.; Voronina, J.K.; Strelnik, A.G.; Vatsadze, S.Z.; Burilov, A.R.; Pudovik, M.A.; Fedorova, O.A.; Sinyashin, O.G. Tandem intramolecular cyclisation/1,3-aryl shift in *N*-(4,4-diethoxybutyl)-1-arylmethanimines (Kazan reaction): Synthesis of 3-benzylidene-1-pyrrolines. *RSC Adv.* **2017**, *7*, 50955–50960. [[CrossRef](#)]
22. Lombardi, B.M.P.; Pezoulas, E.R.; Suvinen, R.A.; Harrison, A.; Dubrawski, Z.S.; Gelfand, B.S.; Tuononen, H.M.; Roesler, R. Bis[cyclic (alkyl)(amino)carbene] isomers: Stable *trans*-bis(CAAC) versus facile olefin formation for *cis*-bis(CAAC). *Chem. Commun.* **2022**, *58*, 6482–6485. [[CrossRef](#)] [[PubMed](#)]
23. Vermersch, F.; Oliveira, L.; Hunter, J.; Soleilhavoup, M.; Jazzar, R.; Bertrand, G. Cyclic (Alkyl)(Amino)Carbenes: Synthesis of Iminium Precursors and Structural Properties. *J. Org. Chem.* **2022**, *87*, 3511–3518. [[CrossRef](#)] [[PubMed](#)]
24. Olguín, J.; Bernès, S.; Gasque, L. Fluoride Ion as Ligand and Hydrogen Bond Acceptor: Crystal Structures of Two Dinuclear Cu^{II} Complexes Built on a Diazecine Template. *Crystals* **2012**, *2*, 1357–1365. [[CrossRef](#)]
25. Sheldrick, G.M. SHELXT—Integrated space-group and crystal-structure determination. *Acta Crystallogr. Sect. A Found. Adv.* **2015**, *A71*, 3–8. [[CrossRef](#)]
26. Sheldrick, G.M. Crystal structure refinement with SHELXL. *Acta Crystallogr. Sect. C Struct. Chem.* **2015**, *C71*, 3–8. [[CrossRef](#)]

Disclaimer/Publisher’s Note: The statements, opinions and data contained in all publications are solely those of the individual author(s) and contributor(s) and not of MDPI and/or the editor(s). MDPI and/or the editor(s) disclaim responsibility for any injury to people or property resulting from any ideas, methods, instructions or products referred to in the content.